Geotextiles and Geomembranes 19 (2001) 387–412
Geotextiles and Geomembranes
www.elsevier.com/locate/geotexmem

Numerical analysis of geosynthetic reinforced retaining wall constructed on a layered soil foundation☆

R. Kerry Rowe*, Graeme D. Skinner

GeoEngineering Centre at Queen's-RMC, Department of Civil Engineering, Queen's University, Ellis Hall, Kingston, Ont., Canada K7L 3N6

Received 1 February 2001; received in revised form 29 April 2001; accepted 10 June 2001

Abstract

A numerical examination of the behaviour of an 8 m high geosynthetic reinforced soil wall constructed on a layered foundation stratum is described. The foundation consists of a 0.8 m hard crust, underlain by 2.95 m of soft loam (sandy/silty) and then 1.3 m of stiff clay. Below the clay is 1.75 m of fine sand underlain by a layer of clayey/fine sand extending to a depth below 10 m. The wall was constructed with 16 segmented concrete facing blocks, a sandy backfill material with 30% fines and 11 layers of geogrid reinforcement 6 m long. Five additional, one metre long layers of reinforcement were used between the 6 m long layers within the upper 5 m of the wall to improve the local stability of the facing blocks. The analysis examines the effect of uncertainty regarding the drained and undrained strength of the loam foundation material, its stiffness, the thickness of this soft layer and its position with respect to the bottom of the wall on the calculated behaviour and compares the calculated and observed behaviour. © 2001 Elsevier Science Ltd. All rights reserved.

Keywords: Geosynthetic; Soil wall; Numerical analysis; Compressible soil; Field case

1. Introduction

The behaviour of geosynthetic reinforced soil walls constructed on a rigid foundation has been extensively investigated both experimentally and theoretically in the past and many current design criteria's are based partly on this research

☆Prof S.A. Tan acted as the Editor coordinating the reviews of this paper.

*Corresponding author. Tel.: +1-613-533-6933; fax: +1-613-533-2126.
E-mail address: kerry@civil.queensu.ca (R. Kerry Rowe).

PII: S0266-1144(01)00014-0

(Bathurst et al., 1988, 1989; Bathurst and Benjamin, 1990; Karpurapu and Bathurst, 1992; Wu, 1992a, b; Ho, 1993; Rowe and Ho, 1993, 1996; Bathurst and Simac, 1994; Michalowski, 1998; Helwany et al., 1999; Porbaha et al., 2000). However, the behaviour of these reinforced soil walls (also called mechanically stabilized walls or MSWs) constructed on soft or yielding foundations has received only limited attention (Bell et al., 1983; Schmertmann et al., 1989; Bergado et al., 1991, 1994; Chou, 1992; Palmeria and Monte, 1997; Otani et al., 1998) and many questions still remain as to the performance and response of these soil structures. It has been previously reported that a yielding foundation can cause an increase in the lateral displacement of the wall facing and the strain in the layers of reinforcement near the bottom of the wall (Palmeria and Monte, 1997; Schmertmann et al., 1989; Chou, 1992). However, the overall behaviour of a MSW constructed on a yielding foundation, including a review of the vertical stress and displacement at the base of the wall, the horizontal stress behind the wall facing and the strain pattern in the reinforcement, has not been examined. This paper investigates the short-term behaviour of a reinforced soil wall constructed on a yielding foundation and analyses the key factors influencing the wall behaviour. The response calculated using a finite element (FE) analysis is compared to the observed behaviour.

The field case investigated was a full-scale test wall constructed at the Public Works Research Institute (PWRI) in Japan (Ochiai and Fukuda, 1996; Nakajima et al., 1996; PWRI, 1997; Tsukada et al., 1998) in the Kanto region of Japan. The 8 m high wall had a concrete block facing and was reinforced with 11 layers of geosynthetic grid reinforcement 6 m long (see Fig. 1). Five additional, one metre long, layers of reinforcement were used between the 6 m long layers within the upper 5 m of the wall to improve the local stability of the facing blocks. The backfill was sand with approximately 30% fines (silty clay). As shown in Fig. 1, the foundation consisted of a 0.8 m thick stiff crust over 2.95 m of soft Kanto loam (sandy silt) over 1.3 m of stiff clay over 1.75 m of fine sand underlain by a layers of clay, fine sand and clayey fine sand extending to a depth of 9.6 m below the base of the wall. Below these layers were various layers of stiff mixed sands. The watertable was at an approximate depth of 4.0 m below the surface of the ground.

A prefabricated concrete key was used at the base of the facing blocks. This was used for alignment purposes only and served no structural purpose. A concrete footing protection block was cast at the toe of the wall at the early stages of construction to prevent the base of the wall from significantly pushing out.

2. Numerical model

A version of the finite element program AFENA (Carter and Balaam, 1990), modified to account for the modelling of reinforced soil walls, was used to conduct the numerical analysis reported herein. The field case was idealized as two-dimensional and a plane-strain analysis was performed. It is acknowledged that this two-dimensional idealization represents an approximation since the wall involves some three-dimensional geometry with a slope perpendicular to the facing at either

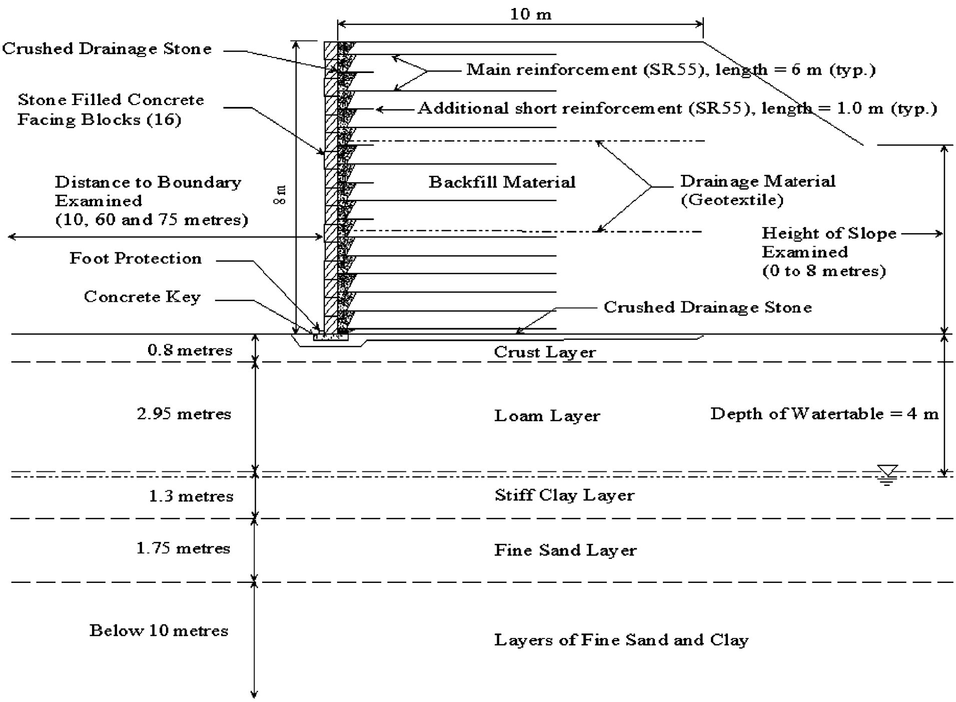

Fig. 1. Cross-section of wall (adapted from PWRI 1997).

end of the wall face (see Fig. 2). However, a two-dimensional analysis was considered to be reasonable for modelling the central section of the wall. A short-term analysis was conducted for the construction of the wall with each soil material being modelled as either drained or undrained depending on its characteristics.

The finite element mesh used 1697 eight noded isoparametric elements to model the soil, concrete and footing block (see Fig. 3), and 1117 interface elements were used between the soil and other materials. The reinforcement was modelled using 417 linear bar elements. The concrete and footing block were treated as elastic materials. An elasto-plastic stress–strain model with a Mohr–Coulomb failure criterion was adopted both for the continuum elements used for the soil and the interface elements between the various materials, as described by Rowe and Soderman (1987). The interface elements are modelled with a stiff spring in each of the shear and normal directions until slip occurred, at which point deformation could occur along the interface and the normal and shear stresses satisfied a Mohr–Coulomb failure criterion. The construction analysis of the wall was conducted layer-by-layer following the sequence described by PWRI (1997). Compaction stresses induced during construction were not accounted for in the analysis.

A limit-equilibrium analysis was conducted to assess the global stability of the wall and foundation. It was found that the deepest point of the slip surface extended to

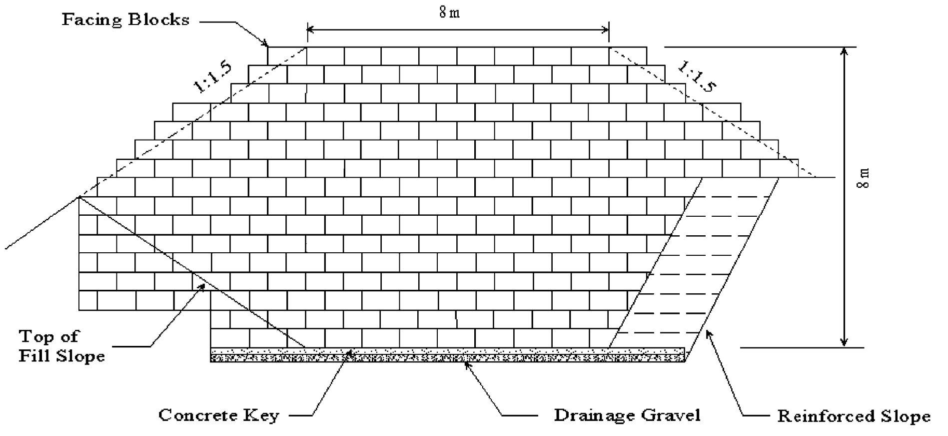

Fig. 2. Front elevation of wall (adapted from PWRI 1997).

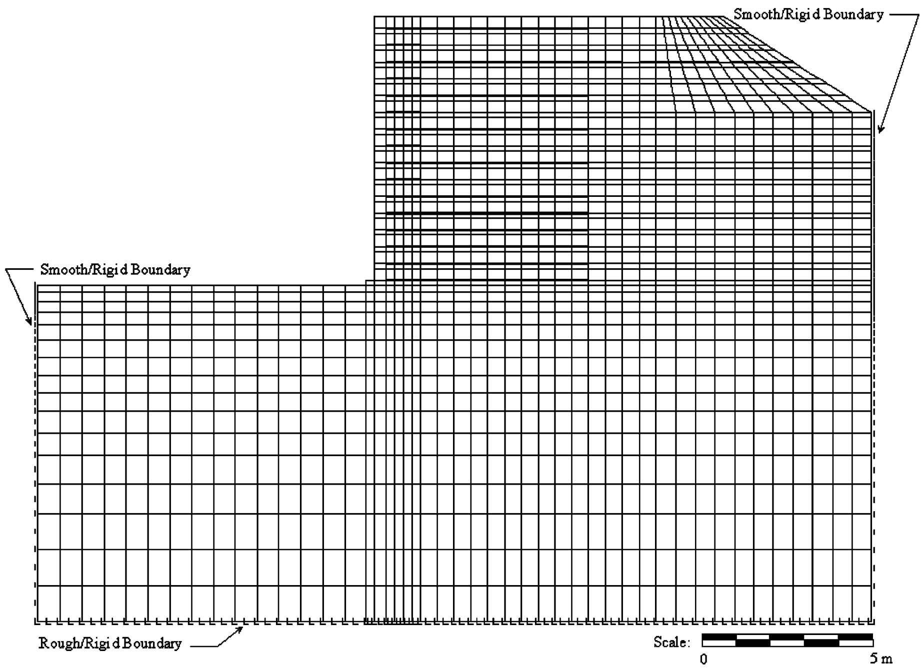

Fig. 3. Finite element mesh.

approximately the middle of the loam layer. Therefore, the foundation was modelled to a total depth of 10 m to ensure an adequate distance from the assumed rough/rigid bottom boundary condition, to the zone of influence due to the construction of the wall.

The right and left boundaries were modelled as smooth rigid for this plane-strain problem. The distance in front of and behind the wall was varied in order to establish the effect of the location of this boundary on the calculated behaviour of the wall. It was found that the response of the wall became insensitive to the location of the boundaries at the front of the wall when this boundary was located 10 m (or more) from the wall face.

The reports (Ochiai and Fukuda, 1996; Nakajima et al., 1996; PWRI, 1997; Tsukada et al., 1998) describing the field test did not clearly define the surface conditions behind the reinforced soil block. From these reports, it was unclear as to whether the 1 : 1.5 slope that starts 4 m behind the reinforced soil mass continues to the elevation of the bottom of the wall or whether it levels out or changes part way down the slope (see Fig. 1). A numerical study was conducted by varying the extent of the slope from zero (no slope) to a complete slope extending to the bottom of the wall (full slope). It was found that the length of the slope had no significant effect on the calculated behaviour of the wall and was therefore far enough away from the reinforced soil block as to have no significant effect on the results. For the analyses reported herein, the slope was extended to a distance of 15 m from the back of the facing blocks as shown in Fig. 3.

3. Model parameters

The various model parameters are given in Table 1. All material properties were based on reported values (Ochiai and Fukuda, 1996; PWRI, 1997) unless indicated otherwise below. The initial geo-static stress condition in the foundation was based on the unit weight of the soil and the effective coefficient of lateral earth pressure at rest (K_0') for each layer. The values of K_0' and Poisson's ratio for the foundation layers were based on empirical correlations with the friction angle of the layer and took into account the over-consolidated nature of the soil using the approach given by Kulhawy and Mayne (1990).

The Young's modulus, E, of all soil parameters, except the stiff clay, was assumed to be given by Janbu's equation $E = K(\sigma_3)^n$ (Janbu, 1963) where the values of K and n were selected based on correlations (Duncan et al., 1980) with the reported soil properties. The stiff clay was assumed to act as a totally saturated, undrained layer with a constant undrained Young's modulus. This undrained modulus was based on an empirical correlation (Kulhawy and Mayne, 1990) accounting for the over-consolidated nature of the clay and its measured plasticity index and undrained shear strength.

It was assumed that the concrete key and footing block were constructed using concrete with a compressive strength (f'_c) of 30 MPa. Based on this value, the Young's modulus was taken according to the empirical correlation $E_c = 4500\sqrt{f'_c}$ from the Canadian Portland Cement Association (1995) and the shear strength of the material was assumed to be 15 MPa. In fact, since the concrete is much stronger and stiffer than the soil materials, the precise values are not especially important and

Table 1
Soil model parameters

Parameter	ϕ' (deg.)	Cohesion (c') (kPa)[a]	Poisson's ratio (ν) (—)	K_0' (—)	Janbu 'n' (—)	Janbu 'K' (—)	Young's modulus (MPa)[a]	Dilation angle (deg.)
Reinforced soil wall								
Backfill	29	1 and 3	0.34	0.52	0.8	50	N/A	0.0
Facing blocks	N/A[b]	30,000	0.15	0.17	N/A[b]	N/A[b]	9800	N/A[b]
Concrete key and footing block	N/A[b]	30,000	0.15	0.17	N/A[b]	N/A[b]	24,000	N/A[b]
Gravel at base of wall	45	0	0.23	0.29	0.7	900	N/A	15.0
Gravel behind face	45	5	0.23	0.29	0.7	1800	N/A	15.0
Geosynthetic	0	29.4[c]	N/A[b]	N/A[b]	N/A[b]	N/A[b]	980[d]	N/A
Foundation								
Crust	35.5	40	0.26	0.74	0.2	1750	N/A[b]	3.0
Loam	35.5	11	0.26	0.74	0.6	200	N/A[b]	3.0
Stiff clay	0	64[e]	0.49	1.10	N/A[b]	N/A[b]	9.630	5.0
Fine sand	30	0	0.35	0.89	0.55	765	N/A[b]	0.0
Clay/Sand	30	10	0.35	0.89	0.3	320	N/A[b]	0.0

[a] Unless otherwise noted below.
[b] N/A—not applicable.
[c] Allowable strength in kN/m in tension only.
[d] Axial stiffness in kN/m width.
[e] Undrained shear strength.

the results of the analysis would not change if the compressive strength and Young's modulus were either higher or lower within the likely range.

It was reported that the backfill consisted of 30% silty and clay particles and unsaturated with the upper portion of the wall having a lower water content and degree of saturation. Based on the work of Fredlund et al. (1995) and Öberg and Sällfors (1995), which showed an increase in the apparent cohesion of a material due to its unsaturated nature, the cohesion intercepts in the bottom and top of the wall were assumed to be 1 and 3 kPa, respectively. The effect of the unsaturated nature of the backfill was only considered in as far as it affected the shear strength of the soil.

It is difficult to determine an approximate dilation angle, ψ', for any of the soils based on the limited known information. The dilation angle of all soil materials was assumed to be given by Bolton's equation $\psi' = (\phi' - \phi'_{cv})/0.8$ (Bolton, 1986) where the value of the constant volume friction angle (ϕ'_{cv}) was assumed to be 33° (Table 1). Except for a slight decrease in the vertical stress at the toe of the wall, the results of an analysis accounting for this dilation were not significantly different from those of a similar analysis assuming no dilation. This small decrease in stress may be have been due to an increase in the stiffness of the gravel at the base of the wall that was confined by the stiff crust and the wall itself and had the highest dilation angle of 15°. The overall analysis and the results presented subsequently assume no dilation.

The crushed stone materials at the base of the wall and behind the wall facing were given different strength and stiffness values to account for the effect of the additional confinement from the reinforcement. It has been shown that the reinforcement of granular soils with geosynthetic material can give rise to an apparent cohesion and increase in stiffness of the granular material (Gorlé and Thijs, 1989; Cazzuffi et al., 1993) relative to the unreinforced material. For example, a gravel material reinforced with geogrid reinforcement, similar to that used in this case, had an apparent cohesion of 22 kPa and an increase in secant stiffness modulus (due to the reinforcement) of approximately 8% for strain values above 5% (Cazzuffi et al., 1993). There was no noticeable increase in stiffness for strain values less then 5%. In the case being examined, the reinforcement was spaced at 0.5 m between the gravel layers and the strain in the reinforcement did not exceed 2%. The local effect was assumed to give rise to an approximate cohesion of 5 kPa and, on average, a doubling of the stiffness along the back of the facing relative to the gravel at the base of the wall. Although the observed strains (2%) were lower than the 5% limit presented by Cazzuffi et al. (1993), the higher strength and stiffness assumed in the gravel behind the wall face lead to horizontal stresses predicted closer to the observed behaviour behind the facing.

Little has been reported about the crust above the loam other than that it was a stiff material with a Young's modulus of 97 MPa (PWRI, 1997) and the published data indicates that the crust consisted of material similar to the loam. Therefore, it was assumed that the crust was a desiccated section of the underlying loam material, and hence, the same friction angle was used for the crust. Due to the desiccated nature of the soil it was assumed that the crust was somewhat fractured and that this fracturing caused the crust to behave in a drained manner. The value of the Poisson's ratio for the crust was based on an empirical correlation with the friction angle using an approach given by Kulhawy and Mayne (1990). The approximate value of K_0' was a little more difficult to estimate when attempting to account for the desiccated nature of the soil. The K_0' could range from 0.74 (same as the loam) to 2.5 (accounting for over-consolidation) as per Kulhawy and Mayne (1990). A parametric study was conducted to examine the effect of varying the K_0' value of the crust and it was found that only the deformation at the base of the wall was noticeably affected. The decrease in settlement at the base caused by increasing the K_0' value was due in part to the increase in the stiffness of the soil materials governed by Janbu's equation (as given above). Even with a K_0' value of 2.5, the stiffness of the loam could be adjusted within an acceptable reported stiffness range to achieve agreement with the observed behaviour. This adjustment did achieve good agreement with the deformation at the toe of the wall, however, there was an increase in the overall deformation below the wall as compared to the results for K_0' equal to 0.74. It was subsequently assumed that the value was the same as the loam layer below it (0.74), since this gave results close to those observed. The crust was given a cohesion value to reflect some increase in strength due to drying, but also allowing for the effect of desiccation on the operational strength as described by Stark and Duncan (1991) and Day and Axten (1989). This increase in the operational strength can be quite significant for some material (Stark and Duncan, 1991) and it was found that an apparent cohesion value of 40 kPa for the crust was the minimum value before excessive deformation, which did not agree with the observed behaviour, was predicted.

The Kanto loam is a volcanic ash loam that was significantly softer than the soil above and below it and consisted of about 74% silt size particles. It has been reported (Japanese Geotechnical Society, 1974), that this material has a relatively high hydraulic conductivity (10^{-4}–10^{-6} m/s), which may have allowed a significant amount of consolidation settlement to occur during the construction phase. This hypothesis is consistent with the nature of observed settlements during and immediately following the construction of the wall and therefore, it was assumed that the loam behaved in a drained manner.

The material properties for the geogrid reinforcement were taken from the reported data (Ochiai and Fukuda, 1996; PWRI, 1997). The connection between the wall and the reinforcement was made in the field by alternately threading steel reinforcement bars through the holes at the end of the geogrid reinforcement sheets. The steel bars and attached geogrid reinforcement were then placed over the top of a second set of steel reinforcement bars that were cast into the back of the wall facing blocks and bent 90° up. For the numerical model, it was assumed that the geosynthetic would fail before the connection and that the backfill would always be moving down past the wall facing panels and therefore the connection would not slip off the top of the bent steel bar and be loose. It was also assumed that the steel poles threaded through the reinforcement sheets could move slightly although the reinforcement bars cast into the wall face and therefore there was no stiffness in the vertical direction of the connection. It is difficult to determine how the connections were actually made and were acting in the field. Some of the connections may have been able to slide up the reinforcement bar (low joint stiffness) and others

Table 2
Interface parameters

Interface materials: (Material 1/Material 2)	Friction angle: (deg.)[a]
Backfill/Reinforcement	29/45[b]
Backfill/Facing	37.5[c]
Backfill/Foundation	23[d]
Facing/Facing	30/22
Facing/Key	30
Key/Foundation	36[d]

[a] Unless otherwise noted below.
[b] Interface friction angle of 45° used for drainage gravel.
[c] Listed as 19°, but found otherwise (see text).
[d] Taken as 80% of maximum friction angle of the weakest material along the interface.

may be sliding into the bend of the bar (high joint stiffness). A parametric study was performed for these two cases and it was found that there was little difference between the two results. Therefore, the joints used to model the connections between the wall face and the geosynthetic layers were not allowed to fail and were given high stiffness in the horizontal direction and very little stiffness in the vertical direction.

The various interface friction angles are given in Table 2. All friction angles were based on reported values unless indicated otherwise below. The interface friction angle between the facing blocks was reported as both 30° and 22°. No significant difference was found when comparing the results from the analyses using both angles. The interface parameters for the key/foundation and backfill/foundation interfaces were based on 80% of the crust and backfill friction angles, respectively. These values were chosen since they were the weaker of the two materials in contact with each other and reduced to 80% to reflect a reasonable reduction in interface strength. The angle of friction between the facing and the backfill gravel was found to give the best results within the range of 30–45°. This range corresponds to an interface angle between $\frac{2}{3}\phi'$ and ϕ' (ϕ' = friction angle) of the gravel. These high interface friction angles are consistent with those reported in other case studies (Bathurst and Simac, 1994). This range and the results of the analysis are discussed in detail in the next section.

4. Comparison of observed and calculated behaviour

The results from the FE analysis, using the above parameters, will be compared to the reported observations from the full-scale test wall (PWRI, 1997). As discussed above, it was found that the analysis gave the best results with facing/backfill interface friction angles between 30° and 45° and corresponding to interface values between $\frac{2}{3}\phi'$ and ϕ'. The results of the analyses using these friction angles, plus the results of an analysis with a facing/backfill interface friction angle of 37.5°, representing the average of the range, are presented below. In the following sections, the deformations at the face and along the base of the wall, the stress along the base of the wall and behind the facing blocks and the strains in various layers of reinforcement were all calculated and compared. All observed data was taken at the time of the end of construction, when the wall was at the full height of 8 m and no significant long-term behaviour had occurred. It should be noted that there is uncertainty associated with many of the parameters used in this study. However, based on the limited data available from the site, the parameters used are considered to represent the best estimate of the in situ soil conditions.

4.1. Deformation and horizontal stress at the wall facing

The calculated and observed deformations at the front of the facing (see Fig. 4) show very encouraging agreement although the deformation was slightly over predicted at the top and bottom of the wall. The wall deformed with a parabolic shape. The maximum displacement occurred at the approximate mid-point of the wall. The jagged shape of the calculated lateral displacement in the upper half of the wall is a consequence of the slight movement of the segmental blocks past one another in the analysis and the exaggerated horizontal scale of Fig. 4. The calculated horizontal displacements were insensitive to the value of the facing/backfill friction angle adopted in the analysis over the range examined because no significant slippage occurred between wall facing and backfill for any of the interface friction angles.

The observed horizontal stress against the back of the wall face was well below the Rankine active pressure conditions calculated for either the backfill material or the drainage gravel. Although this general observation is not uncommon for MSWs

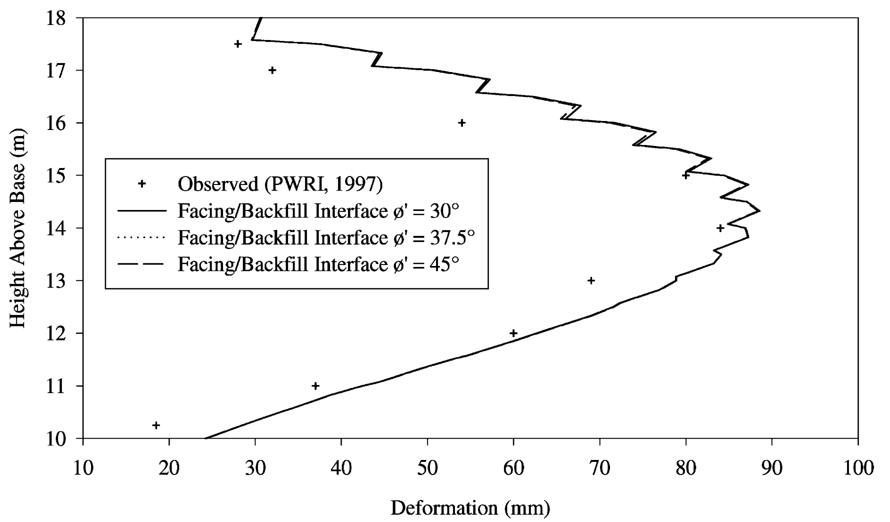

Fig. 4. Comparison of observed and calculated lateral facing deformation.

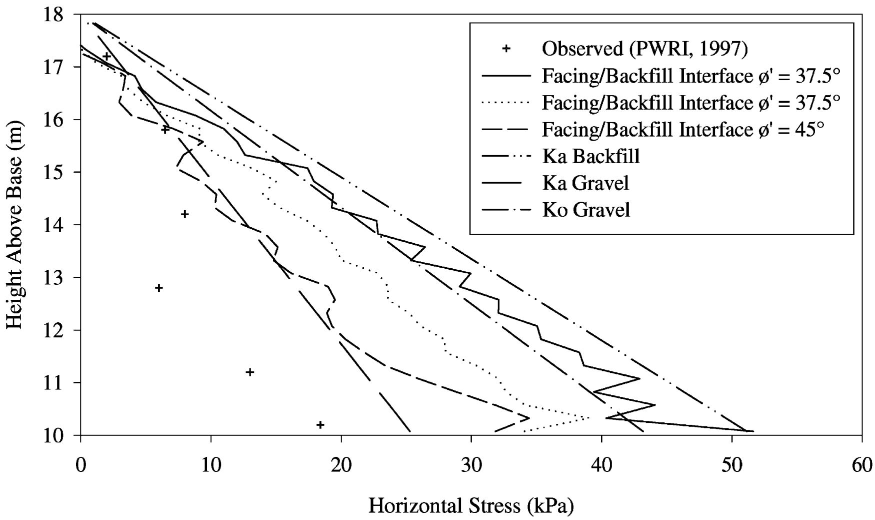

Fig. 5. Comparison of observed and calculated horizontal stress against back of facing.

since other studies have reported horizontal stresses behind the facing that were less than the predicted active earth pressure (Berg et al., 1986; Ho, 1993; Bathurst and Simac, 1994), the pattern of the stress distribution (see Fig. 5) is not consistent with earlier observations and appears somewhat questionable. The results from the FE analysis for three different assumed interface friction angles are shown in Fig. 5. It can be seen that the results fall between the active and at-rest earth pressure conditions for the drainage gravel, with the higher interface friction angle of 45° yielding the lowest horizontal pressure, closest to the observed pressures.

Andrawes and Saad (1999) reported that a vertical compressible layer between the facing and the backfill material could significantly reduce the horizontal stress acting against the back of the facing. Analyses were performed to identify whether the stiffness of the gravel had been overestimated. It was found that although decreasing the stiffness of the gravel layer behind the wall facing did decrease the pressure behind the facing to below the Ka line, the corresponding deformations and stresses at the base of the wall did not agree with the observed results (see Figs. 6 and 7). It was concluded that this was not the explanation for the difference between the predicted and observed horizontal stresses in the lower part of the wall. In another attempt to model the observed low horizontal stress behind the facing, the stiffness of the facing and the interface friction angle between them was decreased. Again, this did not correctly model the full behaviour of the wall.

The observed low horizontal stresses against the wall face could not be reproduced by adjusting the gravel stiffness, the facing stiffness or the facing/backfill interface angles. While it is acknowledged that there may be some other physical explanation that was not captured in the model, it is also considered more likely that there was some error associated with the pressure gauges used to obtain the observed data.

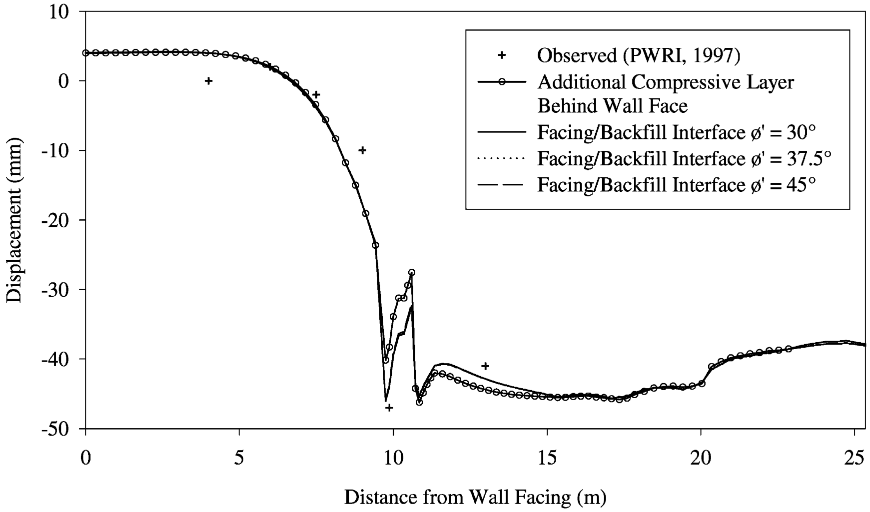

Fig. 6. Comparison of observed and calculated vertical displacement at base of wall.

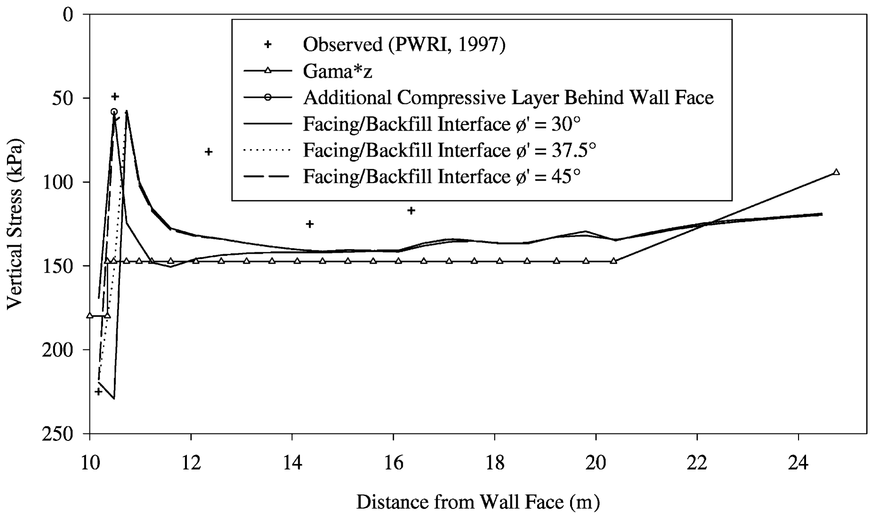

Fig. 7. Comparison of observed and calculated vertical stress at base of wall.

This error may have been due to the location and installation of the pressure gauges on the wall face or in the readings themselves. The gauges were located very close to the connection point of the reinforcement to the wall face and there may have been significant arching and reinforcing effects that occurred at these connections that could cause the measured results to be unrepresentative.

4.2. Deformation and vertical stress at base of wall

The deformations along the surface of the foundation are shown in Fig. 6. The observed and calculated deformations compared well except for the slight difference in front of the wall face. Although the discrepancy was small it was, nevertheless, examined in the parametric study presented below. The study examined the effects of varying the distance from the front of the wall facing to the left boundary, as well as the deformation properties of the loam layer, including anisotropy.

The variation in the calculated displacement along the base of the wall was attributed to the effect of the different stiffness values of the various materials along the base. The deformation was highest at the front toe of the wall. This arose because a portion of the self-weight pressure from the backfill was transferred from the reinforcing and gravel to the wall facing and the wall also rotated slightly increasing the pressure at the toe relative to the heel. This rotation can be seen, highly exaggerated by the distorted scales, in Fig. 6 as the 'spike' in the deformation at the front of the wall.

The observed vertical stresses from the full-scale test wall were less than the self-weight of the wall. This effect was likely due to stress redistribution within the reinforced soil wall. One of the other major features of the vertical stress distribution at the base was the increase in stress at the toe and the decrease in stress towards the heel of the concrete key. As indicated earlier, this is attributed primarily to the rotation of the facing and concrete key, which gave rise to the higher stresses and deformations at the toe. There was a decrease in vertical stress behind the wall due to the transfer of some of the vertical load to the facing as a result of the combined effects of the reinforcement and shear between the backfill and wall face. A similar behaviour (decrease in stress towards the facing) has been observed in other reported cases (Berg et al., 1986; Bathurst et al., 1989; Bathurst and Benjamin, 1990; Allen et al., 1992; Bathurst and Simac, 1994; Ochiai and Fukuda, 1996) and was coupled with an increase in pressure at the toe in a few of these cases (Ochiai and Fukuda, 1996; Allen et al., 1992).

The calculated vertical stress along the base of the wall compared reasonable well with the observed behaviour (see Fig. 7) in terms of the general trend, although the magnitude may have been over-estimated somewhat. The decrease in stress towards the toe, along with the increase in stress at the toe was clearly visible. From Fig. 7, it can also be seen that the stress distribution with an interface friction angle of 30° between the backfill and facing gave results different from the interface friction angle of 45°. The results from the analysis with an interface angle of 30° gave a distribution of vertical stress beneath the wall that was not consistent with those observed. This was due to partial slip along the interface surface. The interface friction angle of 45° gave a result closer to the observed stress behaviour beneath the wall, without any slippage along the interface. From this, it would appear that an interface friction angle of 45° gives better agreement between the calculated and observed results for the vertical stress at the base of the wall. However, the results of the strains in the reinforcement layers must also be considered as discussed below.

4.3. Strain in reinforcement

The reinforcement strains were measured at five levels above the base of the wall: 0.65, 1.65, 3.65, 5.65 and 7.65 m. In each case there was an increase in the strains towards the wall facing, which may be related to the horizontal pressure measured against the back of the wall face. This increase in strain towards the facing has been seen in both laboratory and field studies (Bathurst and Simac, 1994; Krieger et al., 1994; Bergado et al., 1994) where the horizontal stress against the wall facing was also low. The measured strains were all below 1.5% (10.0 kN/m in terms of tensile force) and thus well below the design strength of 29.4 kN/m. The observed and calculated results are shown in Fig. 8. The predicted strains agreed reasonably well with the observed values for the bottom three layers and were slightly higher for the top two layers. This slight over-prediction in strain in the top layers may be attributed to removal of slack in the reinforcement grids in the full-scale wall (PWRI, 1997), as well as error in the measured strain gauges.

It has been reported (Aleksandrov et al., 1988; Brachman, 1999) that the strain measurements for geosynthetic materials have an error associated with the stiffening effect of the strain gauge and, in many cases, are lower than the actual strain. This error is associated with the local reinforcement effect of the foil or wire strain gauge attached to the softer reinforcement material. A correction factor of 1.5 was assumed to be a reasonable value and commonly used in these cases (Aleksandrov et al., 1988; Brachman, 1999). This increase in strain is shown in Fig. 8 as the higher observed strain line (Observed $\times$ 1.5).

The strain results from the interface angle of 30° agreed more closely with the observed behaviour in the lower reinforcement layers than that obtained for the higher interface friction angles. All assumed interface angles showed fairly similar results, except for the drop in strain close to the wall facing in the lower two layers for the two higher interface friction angles that does not agree with the observed behaviour. Therefore, an interface friction angle of 30° was closer to the observed results in this case.

4.4. Summary and conclusions of model wall behaviour

It has been shown that the results of the FE analyses generally compare well with the observed behaviour of the full-scale wall, with a few exceptions. It has been shown that the interface friction angle between the backfill and wall facing had the most noticeable effect on the vertical stress at the toe of the wall and the strains in the reinforcement. The vertical stress was more accurately estimated by the no-slip condition from a friction angle of 45°. The strain in the reinforcement was best estimated by an interface friction angle of 30°, which gave closer results to the observed behaviour in the lower reinforcement layers. It can be concluded that the interface friction angle between the backfill and the wall has a noticeable impact on the vertical stress at the base of the wall and on the strain at the end of the lower reinforcement layers and is somewhere within the range of 30–45° for this case.

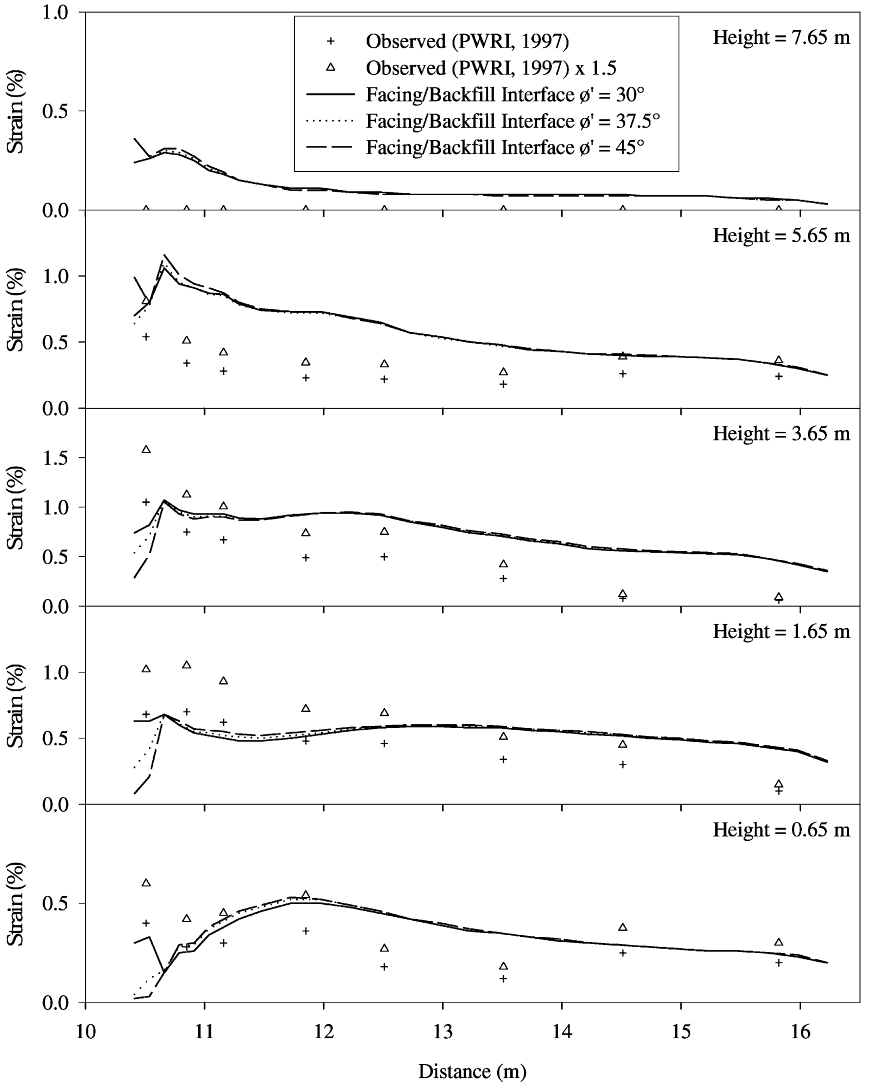

Fig. 8. Comparison of observed and calculated reinforcement strain.

In general, the behaviour of the wall seems to agree with the concept that the loads within the walls are shared with the reinforcement and facing (Bathurst and Simac, 1994). This caused an increase in the deformation and stress at the toe, as well as a decrease in the horizontal pressure against the wall face. The observed strains in the wall all increased towards the facing and were all below the working strain level. For reasons of simplicity and comparison, an average interface friction angle of 37.5° between the facing and backfill material was used for each analysis in the parametric study that follows.

5. Parametric study

A parametric study was conducted to investigate the effect of different characteristics of the soft loam material in the foundation strata. The study was conducted by varying one loam parameter at a time while keeping all other values constant. The various results were then compared to the original baseline case (facing/backfill interface angle of 37.5°). The study examined the effects of varying the drained and undrained strength of the loam, its stiffness, the thickness of the layer and its position with respect to the bottom of the wall. Additional analyses were conducted to examine the effects of varying the distance from the front of the wall face to the far boundary and the results obtained for a yielding foundation compared with those obtained on a rigid foundation.

5.1. Rigid foundation

Since MSWs are normally constructed on a competent foundation, an analysis was conducted to examine how the behaviour of the wall might have been expected to differ had it been built on a rigid foundation. A rough/rigid boundary was placed at the base of the wall and the analysis was conducted with all the wall parameters the same as previous analysis. The general results of the analysis showed that there was significantly less plasticity in the backfill, which behaved essentially elastically during construction, compared to the baseline condition with the compressible foundation. The concrete facing and drainage gravel at the front of the wall interacted together to support the soil mass.

Figs. 9 and 10 show the calculated lateral deformation and horizontal stress at the facing. The maximum horizontal deformation of the wall facing calculated for a rigid base was significantly lower than the baseline results (layered foundation as discussed earlier) and the point of maximum lateral movement occurred higher up the wall (see Fig. 9). The reduction in lateral deformation was, in part, due to lack of movement at the base of the wall since it was restrained at the boundary. The majority of the soil plasticity occurred in the upper section of the wall and this contributed to the larger deformations in this area.

The horizontal pressure in this case was calculated in the sand directly behind the drainage gravel. This was done because it was found that the concrete facing and gravel primarily act together as the wall facing. For the rigid base case, the calculated horizontal stress in the backfill approximately followed Rankine's active condition in the top half of the wall, increased towards the base, and then decreased at the very bottom of the wall (see Fig. 10). For the yielding base case, the calculated horizontal stresses were similar to the rigid base case in the top half of the wall, but then they decreased to less than the active condition towards the base. In both cases, the horizontal stresses corresponded to the lateral displacements of the wall face. In the rigid foundation case, the top half of the wall was behaving under active conditions, while an approximate at-rest condition occurred towards the bottom since it was restrained at the base. For the yielding foundation case, the lateral movement of the entire wall face corresponded to the approximate active stress state acting behind it.

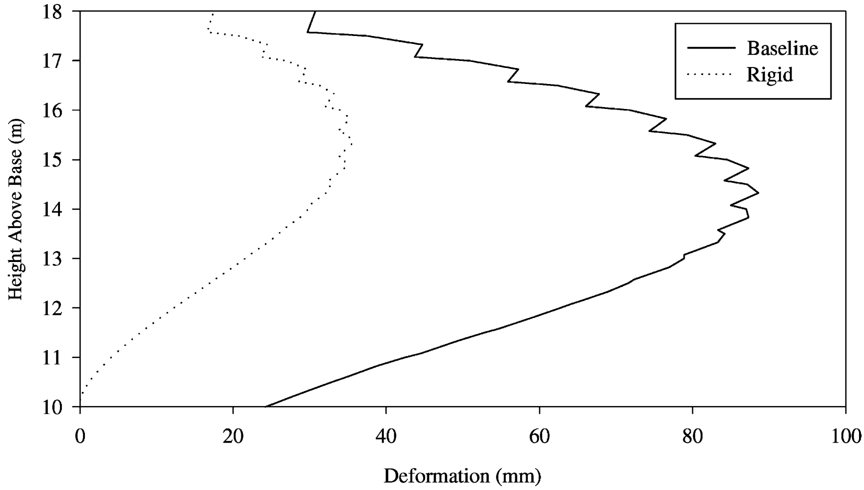

Fig. 9. Comparison of lateral facing deformation for wall on rigid and yielding foundations.

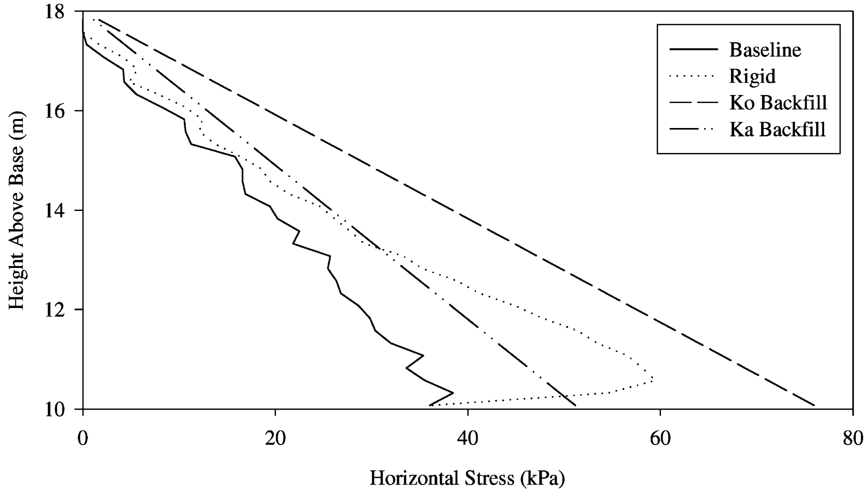

Fig. 10. Comparison of horizontal stresses at back of facing for wall on rigid and yielding foundations.

The vertical stress at the base of the wall followed a similar pattern as the baseline case, except around the toe of the wall. The calculated stress for a rigid foundation was noticeably lower (6%) at the toe than for the baseline case with a compressible foundation. This decrease in stress was likely due to the stress redistribution and rotation at the toe of the wall caused by the rough/rigid foundation at the base.

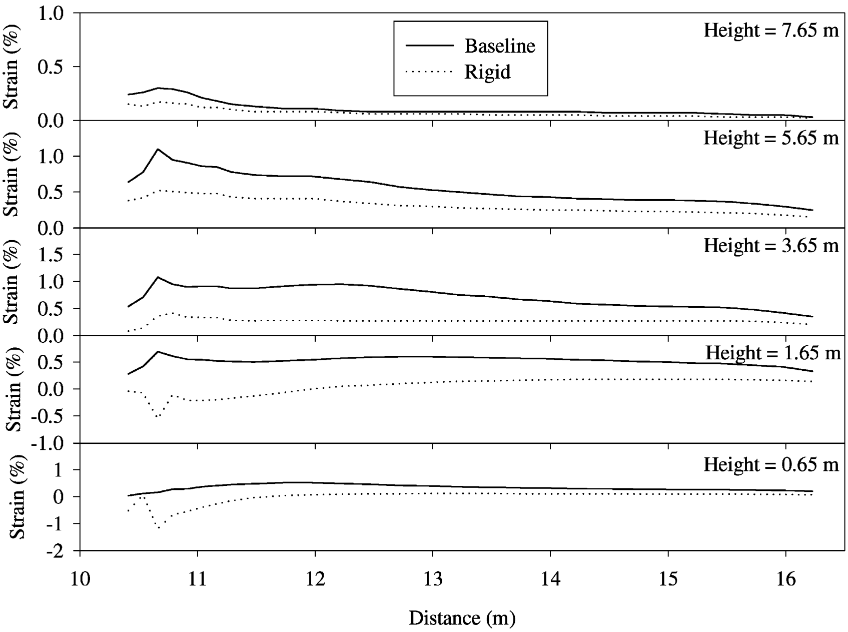

Fig. 11. Comparison of strain in reinforcement layers for wall on rigid and yielding foundations.

The strains in the reinforcement layers were lower than the baseline case at all levels (see Fig. 11) due to stress redistribution in the wall and the decrease in lateral deformation. Compression (negative strain) was found in the two lower measured layers of reinforcement for the rigid case.

5.2. Boundary distance

It was found that extending the distance from the front of the wall face to the far boundary initially from 10 to 60 and 75 m had some effect on the behaviour at the base and front of the wall, but little other effect. The predicted vertical displacement along the top of the foundation, in front of the wall, was found to better conform with the observed behaviour when the boundary was moved out and the analysis better captured the small 'hump' at the toe of the wall (see Fig. 12). Moving the boundary also gave rise to a slight increase in the horizontal displacement of the wall facing, but had little effect on vertical stresses at the base of the wall. The increase in the displacement of the wall face was associated with the slight increase in vertical displacement at the toe of the wall. It can be seen that there was little difference in extending the boundary from 60 to 75 m and therefore, 60 m was found to be an adequate distance to the boundary.

The elastic deformation properties of the loam were also studied to examine their effect on the behaviour of the wall. The Poisson's ratio of the loam was increased

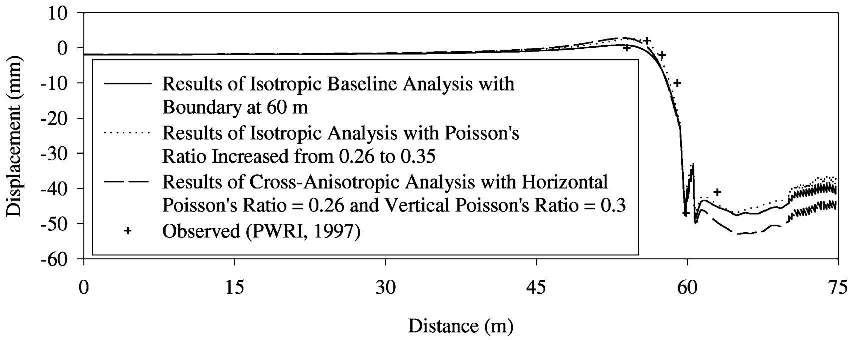

Fig. 12. Vertical deformation at surface of foundation for modified loam parameters with boundary at 60 m.

from the initial estimate of 0.26–0.35 (within the accepted range for this loam material). This change resulted in the predicted vertical displacements at the top of the foundation being slightly closer to the observed behaviour of the wall than the initial analysis (Fig. 12). It was also found that modelling the loam as an elastic cross-anisotropic material with a horizontal Poisson's ratio of 0.26 and a vertical Poisson's ratio of 0.3 resulted in a vertical deformation slightly closer to the observed behaviour then the initial analysis (Fig. 12). These results show that, for the loam, the initial estimate of the Poisson's ratio may be slightly low and there may have been some intrinsic anisotropic behaviour that had not been reported.

5.3. Variation in drained shear strength

The loam had reasonably high drained shear strength values, with a reported apparent cohesion of 11 kPa and a friction angle of 35.5°. For a parametric assessment, the cohesion (c') was set to zero and friction angles (ϕ') of 20° and 28° were examined. The original baseline case ($c' = 11$ kPa and $\phi' = 35.5°$) was used in the comparison and represents the highest strength of the loam. A number of other strength related variables are also examined in the following subsections and results for all these cases are shown in Figs. 13–16.

Decreasing the drained strength of the loam caused an increase in the lateral displacement of the wall face (see Fig. 13). The horizontal stress at the back of the wall face was relatively unchanged, as were the calculated strains in the reinforcement, except for the lowest layer (0.65 m) (see Fig. 15) where there was an increase in strain. Thus, the lowest layer of the reinforcement was most sensitive to changes in the strength of the loam in the foundation. As well as the increase in the lateral displacement of the facing due to decreasing the strength, there was also an increase in the vertical displacement at the toe (see Fig. 16). The stresses at the toe of

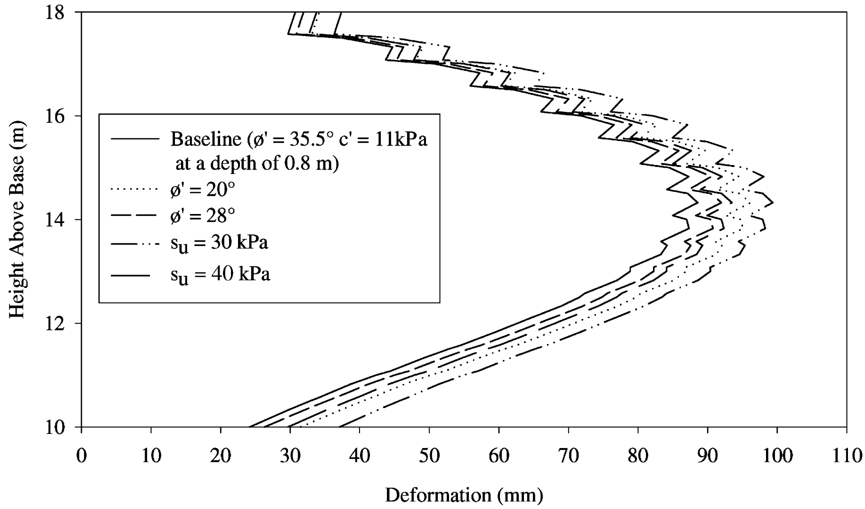

Fig. 13. Lateral wall deformation for various strength values in loam layer.

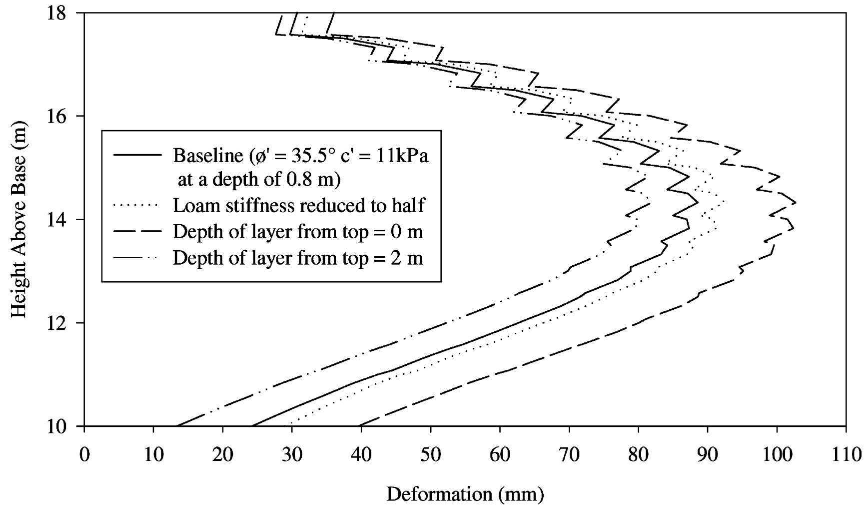

Fig. 14. Lateral wall deformation for various stiffness and depth values in loam layer.

the wall decreased slightly with the decrease in strength, likely due to stress redistribution.

5.4. Variation in undrained shear strength

A review of the undrained strength of the loam was conducted to study its effects on the wall's behaviour. Although the loam appears to have behaved as a drained

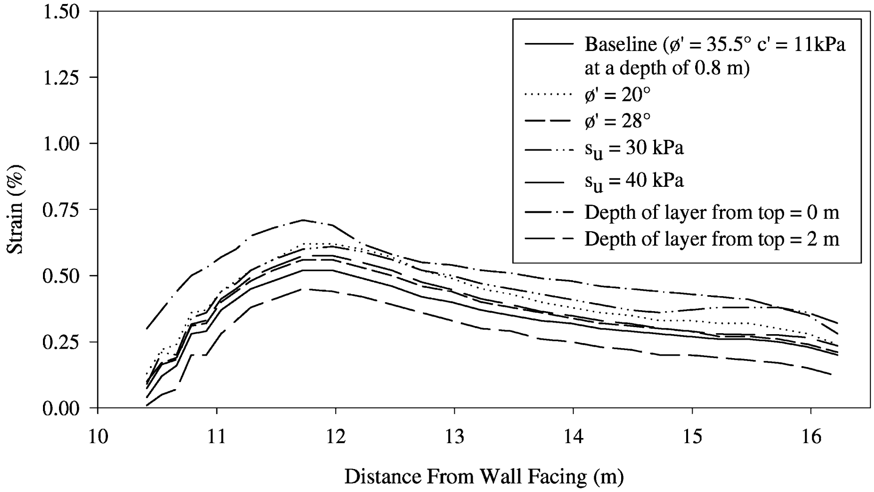

Fig. 15. Stain in reinforcement at height = 0.65 m for various strength, stiffness and depth values in loam layer.

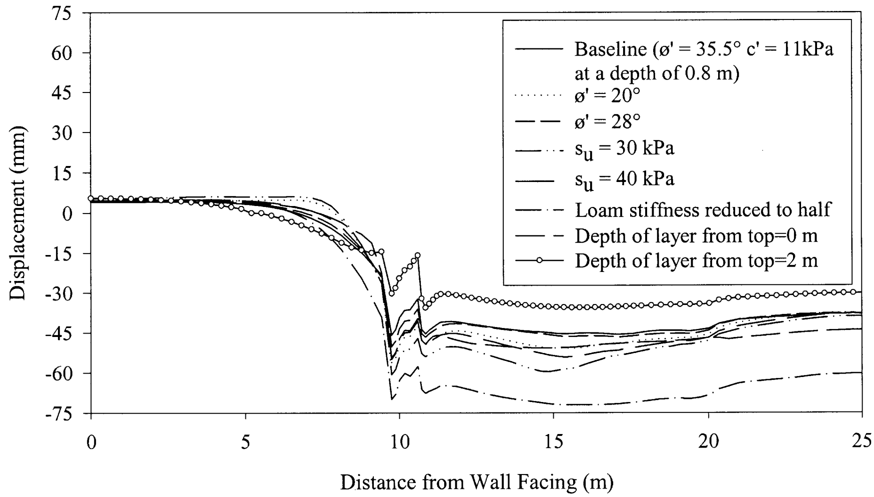

Fig. 16. Vertical deformation at base of wall for various strength, stiffness and depth values in loam layer.

layer, there are many cases where a highly compressible layer is primarily clay and acts in an undrained manner under short-term conditions. Undrained shear strengths of 30 and 40 kPa were examined. It was found that decreasing the undrained strength caused an increase in the deformation of both the facing and the toe of the wall (see Figs. 13 and 16). The horizontal stress against the back of the wall and the strains in the reinforcement were relatively unchanged. This was again with the exception of the lowest measured layer of reinforcement, which showed a slight increase in strain (see Fig. 15).

5.5. Variation of loam stiffness

Although the loam was not particularly stiff, it was of interest to study how the wall may have behaved if the loam had a stiffness of half the baseline conditions examined earlier. Decreasing the loam stiffness only slightly increased the deformation at the face of the wall as compared to the baseline case, but as it might be expected, it significantly increased the settlement at the base (see Figs. 14 and 16). There was a slight decrease in the vertical stress at the toe of the wall and the strains in the reinforcement layers and the horizontal stresses behind the wall were unaffected by the change in loam stiffness.

5.6. Variation of position of loam below wall

A study was conducted to investigate the effects of the position of the loam layer beneath the base of the wall. The loam was initially located 0.8 m below the base of the wall. The position was varied from directly below the wall (0 m) to a position of 2.0 m below the wall's base while its thickness was kept constant (2.95 m). The results showed that as the loam layer was located deeper below the base of the wall, both the maximum deformation of the wall face and the settlement at the base of the wall decreased (see Figs. 14 and 16). Changing the position of the loam had no significant effect on the vertical stress at the base of the wall or the horizontal stress against the back of the wall facing. However, an increase in the strain in the reinforcement in the lower half of the wall was seen when the loam was closer to the base of the wall, as seen in the lowest layer of reinforcement in Fig. 15. This increase in strain was likely due to stress redistribution caused by the compressible layer being closer to the base of the wall. Thus, the further the wall was located from the soft layer, the more the wall behaved like it was constructed on a rigid foundation.

5.7. Conclusions of parametric study

A comparison between the behaviour of a wall with a slightly compressible foundation and a rigid foundation was conducted and showed that, in general, the behaviour can be significantly different. As might be expected, a more compressible foundation can lead to an increase in the deformation at the base of the wall. However, it was also found that construction of a MSW on a soft foundation could cause an increase in the lateral deformation of the wall face, of approximately 150% in this case. As well, it can cause a slight increase in the vertical stress at the toe of the wall and more importantly, an increase in the strains of all measured reinforcement layers. In this case, the strains increased between 80% and over 350%. This behaviour reported herein agrees well with other case studies that show a soft foundation can cause an increase in the facing deformation and strain in the lower reinforcement layers (Schmertmann et al., 1989; Chou, 1992; Palmeria and Monte, 1997).

A parametric study was also used to examine the effects of the properties of the weakest foundation layer. It was concluded that decreasing the strength of the loam material caused an increase in the lateral displacement of the wall face at the mid-point and an increase in the vertical displacement at the toe. As well, the decrease in strength did cause an increase in the strain measured from the lowest measured reinforcement layer. These increases could be due to stress redistribution in the wall.

Decreasing the stiffness of the loam layer caused an increase in the deformation at the base and along the facing of the wall. When the compressible layer was relatively strong, increasing the thickness of the loam layer only affected the settlement at the base of the wall and had no other significant effects on the overall behaviour of the wall.

The position of the soft layer with respect to the base of the wall had a significant effect on its behaviour. When the layer was located close to the base of the wall, the deformations at the face and base of the wall increased, as well as the strains in the reinforcement in the bottom half of the wall. This increase in deformation and strain could have a significant effect on the stability of the wall.

Finally, it was shown that none of the parameters studied in this analysis had any significant effect on the horizontal stress along the back of the facing blocks. Therefore, as one would expect, it can be concluded that the horizontal stress was governed by internal wall parameters and was not significantly affected by the foundation conditions. However, it has been shown that the properties of the drainage material used behind the wall facing can have a significant effect on the behaviour of the wall.

6. Summary and conclusions

A finite element analysis of an experimental full-scale geosynthetic reinforced soil wall has been reported. It was found that the calculated behaviour compared reasonablly well with the observed behaviour of the full-scale wall, with a few exceptions. The interface friction angle between the backfill and wall facing was inferred to be somewhere within the range of interface friction angles of 30–45° for this case.

In general, the behaviour of the wall was consistent with expectations with respect to load distribution, deformation and stress at the toe, horizontal pressure against the wall face and the observed strains in the reinforcement.

It has been shown that for the case of a geosynthetic reinforced soil wall constructed on a yielding foundation, the stiffness and strength of the foundation can have a significant effect on the wall's behaviour. A highly compressible and weak foundation layer can significantly increase the deformations at the wall's face and base, the strains in the reinforcement layers and, to a lesser extent, the vertical stresses at the toe of the wall, compared to a rigid foundation. The only parameter that was not significantly affected by the stiffness or strength of the foundation was the horizontal stresses behind the wall facing.

Acknowledgements

The research report herein was funded by the National Sciences and Engineering Research Council of Canada (NSERC). The authors would like to thank Dr. Hiroshi Miki and Mr. Hijiri Hashimoto of the Public Works Research Institute of Japan and Mr. Tatsuo Iryo from the University of Western Ontario for their assistance in providing and translating reports.

References

Aleksandrov, V.M., Alpaidze, Z.G., Grishin, S.A., Postnikov, B.A., 1988. Strain-gauge measurement error for parts fabricated from low-modulus materials. Izv. AN SSSR., Mekhanika Tverdogo Tela 23 (4), 114–117.

Allen, T.M., Christopher, B.R., Holtz, R.D., 1992. Performance of a 12.6 m high geotextile wall in Seattle Washington. In: Wu, J.T.H. (Ed.), Geosynthetic-Reinforced Soil Walls. Balkema, Rotterdam/Brookfield, pp. 81–100.

Andrawes, K.Z., Saad, M.A., 1999. Geogrid reinforced soil walls subject to controlled lateral deformation. Geosynthetic 1999, Boston, Massachusetts, USA, 28–30 April 1999. Industrial Fabrics Association International, pp. 1–10.

Bathurst, R.J., Benjamin, D.J., 1990. Failure of a geogrid-reinforced soil wall. Transportation Research Record 1288, 109–116.

Bathurst, R.J., Simac, M.R., 1994. Geosynthetic reinforced segmental retaining wall structures in North America. Fifth International Conference on Geotextiles, Geomembranes and Related Products, Singapore, 5–9 September 1994. Southeast Asia Chapter of the International Geotextiles Society, pp. 1275–1298.

Bathurst, R.J., Wawrychuk, W.F., Jarrett, P.M., 1988. Laboratory investigation of two large-scale geogrid reinforced soil walls. In: Jarrett, P.M, McGown, A. (Eds.), The Application of Polymeric Reinforcement in Soil Retaining Structures. Kluwer Academic Publishers, Dordrecht, pp. 71–125.

Bathurst, R.J., Benjamin, D.J., Jarrett, P.M., 1989. An instrumented geogrid reinforced soil wall. Twelfth International Conference on Soil Mechanics and Foundation Engineering, Rio de Janeiro, August 1989. Balkema, Rotterdam/Brookfield, pp. 1223–1226.

Bell, J.R., Barrett, R.K., Ruckman, A.C., 1983. Geotextile earth-reinforced retaining wall tests: Glenwood Canyon, Colorado. Transportation Research Record 916, 59–69.

Berg, R.R., Bonaparte, R., Anderson, R.P., Chouery, V.E., 1986. Design, construction and performance of two geogrid reinforced soil retaining walls. Third International Conference on Geotextiles, Vienna, Austria, 7–11 April 1986. Österreichischer Ingenier-und Architektenverein, pp. 401–406.

Bergado, D.T., Shivashankar, R., Sampaco, C.L., Alfaro, M.C., Anderson, L.R., 1991. Behaviour of a welded wire wall with poor quality, cohesive-friction backfill on soft Bangkok clay: a case study. Canadian Geotechnical Journal 28, 860–880.

Bergado, M.T., Menil N.J.L., Rimoldi, R., Douglas, R.S., 1994. Performance of full scale embankment on soft Bangkok clay with geogrid reinforcement. Fifth International Conference on Geotextiles, Geomembranes and Related Products, Singapore, 5–9 September 1994. Southeast Asia Chapter of the International Geotextiles Society, pp. 1–4.

Bolton, M.D., 1986. The strength and dilatancy of sands. Geotechnique 36 (1), 65–78.

Brachman, R.W.I., 1999. Mechanical performance of landfill leachate collection pipes. Ph.D. Thesis, University of Western Ontario, London, Ontario, Canada.

Canadian Portland Cement Association, 1995. Concrete design handbook, Part II, 2nd Edition. Ottawa, Canada, pp. 1–5.

Carter, J.P., Balaam, N.P., 1990. Program AFENA, A general finite element algorithm. Centre for Geotechnical Research, University of Sydney, New South Wales, Australia.

Cazzuffi, D., Picarelli, L., Ricciuti, A., Rimoldi, P., 1993. Laboratory investigations on the shear strength of geogrid reinforced soils. ASTM special technical publication 1190: geosynthetic soil reinforcement testing procedures, pp. 119–137.

Chou, N.N.S., 1992. Performance of geosynthetic reinforced soil walls. Ph.D. Thesis, University of Colorado at Boulder, Boulder, Colorado, U.S.A.

Day, R.W., Axten, G.W., 1989. Surficial stability of compacted clay slopes. Journal of Geotechnical Engineering 115 (4), 577–580.

Duncan, J.M., Byrne, P., Wong, K.S., Mabry, P., 1980. Strength, stress-strain and bulk modulus parameters for finite element analysis of stresses and movement in soil masses. College of Engineering, University of California, Berkeley.

Fredlund, D.G., Vanapalli, S.K., Xing, A., Pufahl, D.E., 1995. Predicting the shear strength function for unsaturated soils using the soil-water characteristic curve. First International Conference on Unsaturated Soils, Paris, France, 6–8 September 1995. Balkema, Rotterdam/Brookfield, pp. 63–69.

Gorlé, D., Thijs, M., 1989. Geosynthetic-reinforced granular materials. Twelfth International Conference on Soil Mechanics and Foundation Engineering, Rio de Janeiro, August 1989. Balkema, Rotterdam/Brookfield, pp. 715–718.

Helwany, S.M.B., Reardon, G., Wu, J.T.H., 1999. Effects of backfill on the performance of GRS retaining walls. Geotextiles and Geomembranes 17 (1), 1–16.

Ho, S.K.P., 1993. A numerical investigation into the behaviour of reinforced soil walls. Ph.D. Thesis, The University of Western Ontario, London, Ontario, Canada.

Janbu, N., 1963. Soil Compressibility as determined by oedometer and triaxial tests. European Conference of Soil Mechanics and Foundation Engineering, Wiesbaden, pp. 19–25.

Japanese Geotechnical Society, 1974. Problematic soil in Japan. Japanese Geotechnical Society, pp. 22–83 (in Japanese).

Karpurapu, K., Bathurst, R.J., 1992. Analysis of geosynthetic reinforced soil wall by the finite element method. Fourth International Conference on Numerical Models in Geomechanics: NUMOG 4, Swansea, U.K., 24–27 August 1992. Balkema, Rotterdam/Brookfield, pp. 861–870.

Krieger, J., Erban, P.J., Thamm, B.R., 1994. Numerical analysis of full-scale tests on geosynthetic reinforced retaining walls. International Journal of Computer Application in Technology 7 (3–6), 242–250.

Kulhawy, F.H., Mayne, P.W., 1990. Manual on estimating soil properties for foundation design. Research Project 1493-6, Cornell University, Ithaca, New York.

Michalowski, R.L., 1998. Limit analysis in stability calculations of reinforced soil structures. Geotextiles and Geomembranes 16 (6), 311–331.

Nakajima, T., Toriumi, N., Shintani, H., Miyataka, H., Dobahi, K., 1996. Field performance of a geotextile reinforced soil wall with concrete facing blocks. In: Ochiai, H., Yasufuku, N., Omine, K. (Eds.), Earth Reinforcement. Balkema, Rotterdam/Brookfield, pp. 427–432.

Öberg, A.L., Sällfors, G., 1995. A rational approach to the determination of the shear strength parameters of unsaturated soils. First International Conference on Unsaturated Soils, Paris, France, 6–8 September 1995. Balkema, Rotterdam/Brookfield, pp. 151–158.

Ochiai, Y., Fukuda, N., 1996. Experimental study on geotextile-reinforced soil walls with different facing. In: de Groot, M.B., de Hoedt, G., Termaat, R.J. (Eds.), Symposium on Geosynthetics: Application, Design and Construction. Balkema, Rotterdam/Brookfield, pp. 113–120.

Otani, J., Hirai, T., Ochiai, H., Shinowaki, S., 1998. Evaluation of foundation support for geosynthetic reinforced soil wall on sloping ground. Sixth International Conference on Geosynthetics, Atlanta, USA, 25–29 March 1998. Industrial Fabrics Association International, pp. 601–603.

Palmeria, E.M., Monte, L.M., 1997. The behaviour of model reinforced walls on soft soils. Geosynthetics '97, Long Beach California, USA, 11–13 March 1997. Industrial Fabrics Association International, pp. 73–84.

Porbaha, A., Zhao, A., Kobayashi, M., Tishida, T., 2000. Upper bound estimate of scaled reinforced retaining walls. Geotextiles and Geomembranes 18 (6), 403–413.

Public Works Research Institute (PWRI), 1997. Observation of behaviour of full scale model test on reinforced retaining wall using geotextile. PWRI, Japan, Report #3487.

Rowe, R.K., Ho, S.K.P., 1993. A review of the behaviour of reinforced soil walls. In: Ochiai, H., Hayashi, S., Otani, J. (Eds.), Earth Reinforcement. Balkema, Rotterdam/Brookfield, pp. 801–830.

Rowe, R.K., Ho, S.K.P., 1996. Some insights into reinforced wall behaviour on finite element analysis. In: Ochiai, H., Yasufuku, N., Omine, K. (Eds.), Earth Reinforcement. Balkema, Rotterdam/Brookfield, pp. 485–490.

Rowe, R.K., Soderman, K.L., 1987. Stabilization of very soft soils using high strength geosynthetics: the role of finite element analysis. Geotextiles and Geomembranes 6 (1–3), 53–80.

Schmertmann, G.R., Chew, S.H., Mitchell, J.K., 1989. Finite element modelling of reinforced soil wall behaviour. Department of Civil Engineering, University of California, Berkeley, Geotechnical Engineering Report No. UCB/GT/89-01.

Stark, T.D., Duncan, J.M., 1991. Mechanisms of strength loss in stiff clay. Journal of Geotechnical Engineering 117 (1), 139–154.

Tsukada, Y., Ochiai, Y., Miyataka, H., Tajiri, 1998. Field performance of a geosynthetic-reinforced soil wall with rigid facing. Sixth International Conference on Geosynthetics, Atlanta, USA, 25–29 March 1998. Industrial Fabrics Association International, pp. 577–580.

Wu, J.T.H., 1992a. Measured behaviour of the Denver walls. International Symposium on Geosynthetic-Reinforced Soil Walls, Denver, Colorado, USA, 8–9 August 1991. Balkema, Rotterdam/Brookfield, pp. 31–42.

Wu, J.T.H., 1992b. Predicting performance of the Denver walls: General Report. International Symposium on Geosynthetic-Reinforced Soil Walls, Denver, Colorado, USA, 8–9 August 1991. Balkema, Rotterdam/Brookfield, pp. 3–20.